

---

## INFLUENCE OF CHARGE CARRIER THERMAL ACTIVATION ON THE TEMPERATURE DEPENDENCES OF DARK CURRENT, PHOTOCONDUCTIVITY, AND PHOTOLUMINESCENCE IN $\text{In}_{0.4}\text{Ga}_{0.6}\text{As}/\text{GaAs}$ HETEROSTRUCTURES WITH QUANTUM DOTS

O.V. VAKULENKO,<sup>1</sup> S.L. GOLOVYNSKYI,<sup>1</sup> S.V. KONDRATENKO,<sup>1</sup> I.A. GRYN,<sup>1</sup> V.V. STRELCHUK<sup>2</sup>

<sup>1</sup>Taras Shevchenko National University of Kyiv, Faculty of Physics  
(2, Academician Glushkov Ave., Kyiv 03022, Ukraine; e-mail: [golovinskiy.serg@gmail.com](mailto:golovinskiy.serg@gmail.com))

<sup>2</sup>V. Lashkaryov Institute of Semiconductor Physics, Nat. Acad. of Sci. of Ukraine  
(41, Prosp. Nauky, Kyiv 03680, Ukraine)

PACS 73.63Kv, 73.21La,  
78.67Hc, 71.55Eq, 78.55Cr,  
78.56-a, 72.40+w  
©2011

---

The  $\text{In}_{0.4}\text{Ga}_{0.6}\text{As}/\text{GaAs}$  heterostructure with quantum-dot chains has been studied. Dark current measurements reveal the anisotropy of electrical properties of the structure in the temperature range 77–150 K. The wave-function damping length and the average hopping distance in the heterostructure are calculated. The energy diagram of the heterosystem is analyzed by using the lateral photocurrent and photoluminescence spectroscopies. The activation energies of electrons and heavy holes were determined from experimental data in the framework of a theoretical model proposed for the temperature dependence of the lateral photocurrent.

using absorption spectroscopy [5, 6], photoluminescence (PL) [7, 8], and Raman spectroscopy [9].

The features of the electron spectrum and the longitudinal motion of charge carriers in such heterostructures allow the latter to be used as a basis for the creation of infra-red photodetectors and photoresistors with quantum-sized objects in the active region, in which the interband and interlevel transitions are engaged. In particular, photodetectors with  $\text{InGaAs}$  QDs were developed, which are photosensitive in the medium (3–5  $\mu\text{m}$ ) and far (8–14  $\mu\text{m}$ ) infra-red ranges [10–12]. In works [13, 14], the generation of a photocurrent and a photoemf in lateral structures, in which a photoexcited current carrier has to overcome a  $\text{GaAs}$  barrier to reach the contacts, has been studied. In researches of the lateral photocurrent, localized nonequilibrium charge carriers have to be excited to a two-dimensional wetting layer (WL), in which the transport of charge carriers is possible along the direction of an applied weak electric field. The escape of the charge carriers localized in QDs takes place as a result of either their band-to-continuum transitions [15] or the processes of thermally induced emission.

The processes of thermal emission and capture of charge carriers by localized states in QDs substantially affect the longitudinal transport and the recombination phenomena in and the photosensitivity of quantum-sized heterostructures of type I [16]. The understanding of

### 1. Introduction

Semiconductor heterostructures with quantum dots (QDs) and quantum threads demonstrate unique fundamental properties owing to the quantum-mechanical size effects, which is promising for the application of those objects in nanoelectronics. On the basis of low-dimensional heterostructures of type I, novel optoelectronic devices have been created. The  $\text{InAs}$  QDs in  $\text{GaAs}$  matrices were used as an active medium in infra-red lasers [1], as well as a material for optical information storage devices [2] and novel single-electron [3] and quantum-information facilities [4]. A considerable number of publications were devoted to the study of optical properties of  $\text{InGaAs}/\text{GaAs}$  heterostructures with QDs

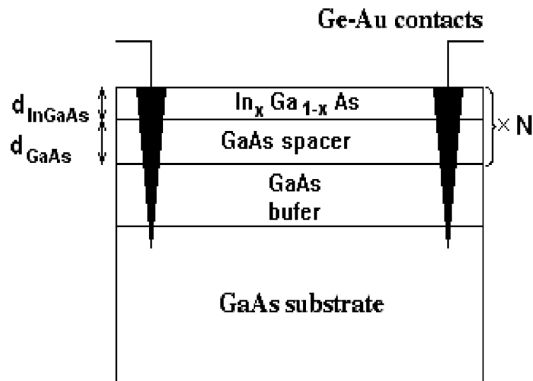


Fig. 1. Schematic diagram of specimens with InGaAs quantum dots and the geometry of eutectic Ge–Au contacts

the temperature dependences of the charge carrier emission processes from QD levels will allow the mechanism of photosensitivity and the factors that restrict the efficiency of InGaAs/GaAs-based photodetectors to be elucidated. We tried to comprehend the role of the charge carrier capture at localized and delocalized states in QDs in the lateral photocurrent generation.

This work aimed at studying the influence of thermal emission processes on the temperature dependences of the lateral dark current (DC), lateral photoconductivity (LPC), and PL in  $\text{In}_{0.4}\text{Ga}_{0.6}\text{As}/\text{GaAs}$  heterostructures with quantum dots. The researches were also aimed at comparing between the dark conductivity and the photoconductivity in the cases where the electric field was applied either along or across the QD chains. By analyzing the shape of the obtained temperature and spectral dependences, we determined the activation energies for the processes of thermally induced electron and hole emission from the QD states, as well as the electron spectrum of heterostructures under investigation.

## 2. Experimental Part

Multilayered low-dimensional  $\text{In}_{0.4}\text{Ga}_{0.6}\text{As}/\text{GaAs}$  heterostructures to study were grown up using the method of molecular beam epitaxy. To eliminate defects, the GaAs(100) substrate was covered with a GaAs buffer layer. An  $\text{In}_{0.4}\text{Ga}_{0.6}\text{As}$  layer of the thickness  $d_{\text{InGaAs}} = 4$  nm was grown up on the GaAs buffer and covered with a thin GaAs layer of the thickness  $d_{\text{GaAs}} = 38$  nm. This procedure was repeated 17 times (Fig. 1). The  $\text{In}_{0.4}\text{Ga}_{0.6}\text{As}/\text{GaAs}$  structures were so grown up that the QDs had a chain-like arrangement. The average distance between the QD chains was 90 nm. The topograms (Fig. 2) registered on a Ntegra (NT–MDT) atomic-power microscope were analyzed to obtain the

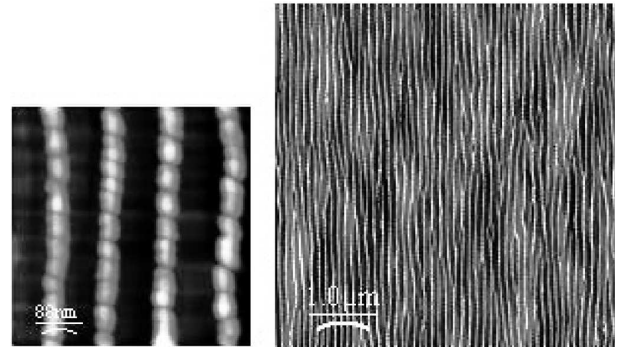


Fig. 2. AFM images of the surface layer of the  $\text{In}_{0.4}\text{Ga}_{0.6}\text{As}/\text{GaAs}$  heterostructure

surface concentration of QDs, which amounted to about  $2 \times 10^{10} \text{ cm}^{-2}$ , as well as their average width (48 nm) and height ( $\approx 7$  nm).

For experiments, we prepared specimens with two different arrangements of contacts, oriented in parallel and perpendicularly to the QD chain direction in the specimen. Such geometries of contact arrangement ensured that the current runs through the specimen in either of two mutually orthogonal directions, along the QD chains or perpendicularly to them. Ohmic contacts 0.6 mm in diameter which are located at a distance of 3 mm from each other were formed on the basis of Au–Ge eutectic alloy on the surface of specimens with epitaxial layers. As a result, the ohmic contacts with every epitaxial layer and the GaAs substrate were provided (Fig. 1).

The DC and photocurrent measurements were carried out using a current amplifier and a standard technique of detection of a constant photocurrent in the temperature range from 77 to 290 K. The voltage  $U = 16$  V was applied to the specimen.

To study the optical transitions under LPC conditions, we applied the method of photocurrent spectroscopy in the geometry where the exciting radiation fell normally onto the surface. The spectral LPC dependences were measured on an infra-red spectrometer in the energy range from 0.8 to 1.6 eV. The obtained spectral dependences of the photocurrent were normalized to a constant number of exciting radiation quanta with the help of a non-selective pyroelectric detector.

PL measurements were carried out following the standard technique on an infra-red spectrometer and in the same energy range  $h\nu = 0.8 \div 1.6$  eV. Excitation was carried out using a laser with a wavelength of 404 nm and a power of  $5 \text{ W/cm}^2$ . The spectral width of a slit in this measurement range was 17 meV. The specimen temperature was 77 K. A cooled Ge photodetector was used for the radiation registration.

### 3. Results and Their Discussion

#### 3.1. Dark current measurements

In Fig. 3, the temperature dependences of DC at an identical bias voltage of 16 V applied perpendicularly to the QD chains (a dotted curve) and along them (a solid curve) are depicted. The largest differences between them are observed within the temperature interval ranging from 77 to 150 K, when the conductivity of wide-band-gap GaAs is low, and the charge carriers mainly move along the layers with QD and WL, which are characterized by a higher equilibrium concentration of charge carriers. Different temperature dependences were observed in this temperature range, which points to different mechanisms of charge carrier transport, i.e. to the anisotropy of electric properties.

At low temperatures, the transport of charge carriers is substantially affected by the processes of thermal emission and capture of charge carriers in the potential wells of InGaAs QDs. Namely, the charge carriers, after their thermally assisted escape from the potential well into delocalized states of barrier levels, drift toward the contacts and find themselves in the field of the next well which is capable to capture them. After being captured by the potential well, the charge carriers can be thermally activated to transit again into the delocalized state. The processes of recapturing and thermal emission are repeated as the charge carriers move toward the contacts. Such a hopping mechanism of charge transfer is described in works, where the conductivity in nanofilms, as well as heterosystems of type II, were studied [17–19]. In the low-temperature interval ranging from 77 to 150 K, the temperature dependence of the conductivity in the case where the charge carriers drift along QD chains can be described by the expression

$$I_{DC} \sim \sigma = \sigma_0 \exp \left[ - \left( \frac{T_{ES}}{T} \right)^{0,5} \right]. \quad (1)$$

Hence, the so-called “1/2 law” is obeyed. It is predicted both in the Efros–Shklovskii model of hopping conductivity with a variable hopping length [20] and in the Mott model for the one-dimensional (1D) case where the electron motion is quantized in two directions. However, to substantiate the one-dimensionality of the examined system for actual sizes of QDs is a difficult task. The average lateral size of nanoislands is 40 nm, i.e. the condition for the charge carrier motion quantization is satisfied in one direction only; it is the direction of growth.

Adopting the Efros–Shklovskii model as a basis, we carried out calculations admissible for the structure con-

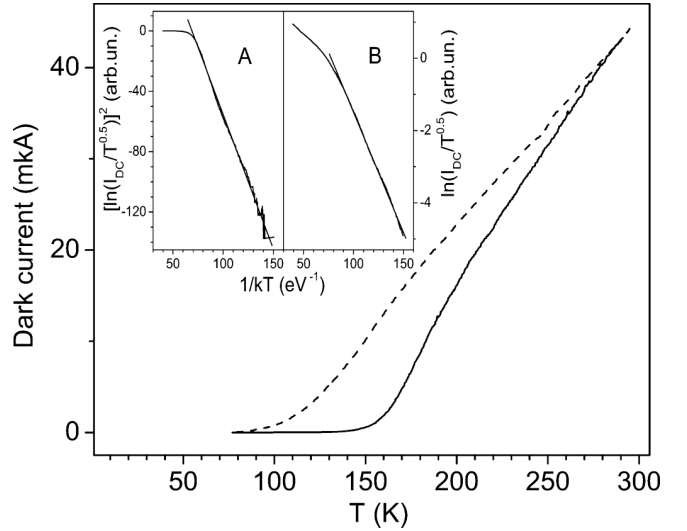


Fig. 3. Temperature dependences of DC in  $\text{In}_{0.4}\text{Ga}_{0.6}\text{As}/\text{GaAs}$  heterostructures in the temperature range from 77 to 290 K with the contacts oriented in parallel (solid curve) or perpendicularly (dashed curve) to QD chains. The insets show the same dependences in logarithmic coordinates for the parallel (A) and perpendicular (B) contact geometries

cerned. In particular, in formula (1),  $T_{ES} = \frac{1}{4\pi\epsilon_0\epsilon} \frac{C e^2}{k_B \xi}$ , where  $\xi$  is the wave function localization radius,  $k_B$  the Boltzmann constant,  $e$  the electron charge, and  $C$  a numerical coefficient depending on the structure dimensionality [20]. The theoretical value of the constant  $C$  for the two-dimensional (2D) model of particle capture, if the recapture is not considered, is  $C = 6.2$  [20]. The dielectric permittivity of InGaAs is  $\epsilon = 13.1$ .

The parameter  $\sigma_0$  is not a constant for the majority of structures, depending on the charge carrier concentration at localization levels which are engaged into the conductivity. In turn, the concentration of charge carriers is a function of the temperature. As a result, the general form of the  $\sigma_0(T)$ -dependence looks like [21]

$$\sigma_0 = \gamma T^m, \quad (2)$$

where  $\gamma$  is a parameter independent of the temperature. In Fig. 3 (inset A), the temperature dependence of the dark current plotted in the coordinates  $\ln^2(I_{DC}/T^{0.5})$  versus  $(k_B T)^{-1}$  is depicted. In those coordinates, the straight line with the slope  $m = 0.5$  was obtained in the temperature interval from 77 to 150 K. The tangent of the slope angle of this straight line was used to calculate the parameter  $T_{ES} = 15500$  K and the wave function localization radius  $\xi = 0.5$  nm.

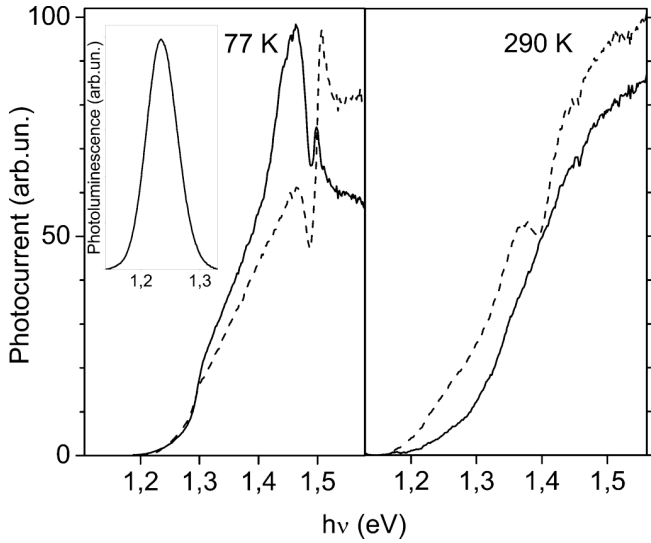


Fig. 4. LPC spectra of  $\text{In}_{0.4}\text{Ga}_{0.6}\text{As}/\text{GaAs}$  heterostructures with the geometries of contacts in parallel (solid curve) and perpendicularly (dashed curve) to a QD at 77 and 290 K. The PL spectrum obtained at 77 K is shown in the inset

The average hopping distance is [21]

$$r_h = \frac{\xi}{4} \left( \frac{T_{ES}}{T} \right)^{0,5} \quad (3)$$

We used the values obtained for  $\xi$  and  $T_{ES}$  in the temperature range 77–150 K to calculate the hopping distance  $r_h = 1.25 \div 1.75$  nm. This magnitude is comparable with the distance between the edges of neighbor nanoislands. As is seen from the AFM images of the upper heterostructure layer, the distance between the neighbor QD chains is about 90 nm which is much larger than the average hopping distance in this structure.

If the electric field is applied perpendicularly to the chain direction, another conductivity mechanism, different from the hopping one, is realized. In the concerned temperature interval 77–150 K, the temperature dependence of DC demonstrates the activation character (Fig. 3). The curve shape is governed by the processes of thermal emission, taking into account the temperature-induced variations of the charge carrier concentration in the states of InGaAs QDs,

$$I_{DC} \sim T^y \exp \left( -\frac{E_a}{k_B T} \right), \quad (4)$$

where  $E_a$  is the activation energy of charge carriers. In Fig. 3 (inset B), the temperature dependence of the dark current plotted in the coordinates  $\ln(I_{DC}/T^{0.5})$  versus  $(k_B T)^{-1}$  is exhibited. In those coordinates, the straight

line with  $y = 0.5$  and  $E_a = 70 \pm 10$  meV was obtained. In our case, the obtained value  $y = 0.5$  corresponds to a dependence typical of the quantum well. The obtained value for  $E_a$  is the activation energy of majority carriers in the heterosystem.

As the temperature grows from 150 to 290 K, the dark current curves for both specimens change their shapes. Such a behavior can be explained by the fact that the capture of charge carriers onto localized states is less probable at high temperatures, so that only the scattering of charge carriers by QDs takes place. In addition, the temperature growth results in an acceleration of the rate of charge carrier thermal generation in the intermediate GaAs layers and the WL, which makes their conductivity higher and, using the QDs, shunts the current.

### 3.2. Photocurrent and photoluminescence measurements

The LPC spectral dependences for the  $\text{In}_{0.4}\text{Ga}_{0.6}\text{As}/\text{GaAs}$  heterostructure measured at room temperature and at 77 K are depicted in Fig. 4. The minimal energy of quanta that stimulated the photocurrent was  $1.17 \pm 0.01$  eV at room temperature and  $1.22 \pm 0.01$  eV at 77 K. In the spectral interval, where crystalline GaAs is transparent ( $h\nu < 1.43$  eV at 290 K and  $h\nu < 1.51$  eV at 77 K), the nonequilibrium charge carriers are generated as a result of interband optical transitions with the assistance of states in nano-sized InGaAs QDs or in the wetting layer. Depending on the dimensions of InGaAs QDs and the In content in them, the number and the arrangement of levels in the quantum well are changed [4]. According to the results of our calculations, the examined structure had one level of quantization for electrons in the QD conduction band ( $E_{e1}$ ) and two levels of quantization for heavy holes (hh) in the QD valence band ( $E_{hh1}$  and  $E_{hh2}$ ).

The energy of transitions, which is observed in the LPC spectra and corresponds to transitions, in which the ground states of QDs participate, amounts to  $1.22 \pm 0.01$  eV at 77 K (Fig. 4). The growth of a LPC signal starting from an energy of  $1.30 \pm 0.01$  eV corresponds to transitions in QDs, in which the excited states are engaged. In the energy interval from 1.22 to 1.51 eV, we observe two maxima which correspond to the transitions from the levels of heavy and light holes into the WL [22]. The positions of the maxima correspond to  $E_{hh}^{WL} = 1.46 \pm 0.01$  eV and  $E_{lh}^{WL} = 1.50 \pm 0.01$  eV, so that the splitting of the WL level into heavy- and light-hole (lh) levels amounts to 40 meV.

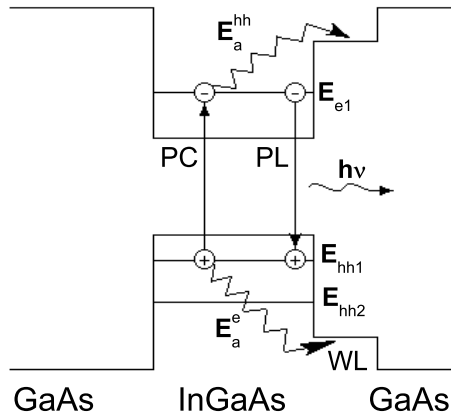


Fig. 5. Energy diagram of the  $\text{In}_{0.4}\text{Ga}_{0.6}\text{As}/\text{GaAs}$  heterostructure

The shape of the LPC spectrum obtained at 290 K differs from that obtained at 77 K (Fig. 4). At room temperature, a sharp growth of the photosensitivity was observed at  $1.17 \pm 0.01$  eV, which corresponds to the interband transition energy with the participation of ground QD states. The energy of the basic transition  $E_{hh-e1}$  is known to diminish as the temperature increases [1]. The difference between the energies of the basic transition  $E_{hh-e1}$  in the QD at 77 and 290 K is equal to 50 meV. A further increase of the photocurrent signal at energies higher than  $1.28 \pm 0.01$  eV corresponds to interband transitions in QDs with the participation of excited states. The LPC spectrum also allows one to obtain the energy of transition from the heavy-hole level in the WL,  $E_{hh}^{WL} = 1.37 \pm 0.01$  eV, which corresponds to the LPC maximum. The contribution given by the light-hole levels in the WL cannot be separated.

Figure 4 (the inset) demonstrates the PL spectrum of the  $\text{In}_{0.4}\text{Ga}_{0.6}\text{As}/\text{GaAs}$  heterostructure with QDs obtained at 77 K. The PL researches revealed a radiative recombination transition only with the participation of ground QD states  $E_{hh1}$  and  $E_{e1}$ . The maximum of the PL peak corresponds to an energy of  $1.235 \pm 0.01$  eV. This value is the energy of the transition from the QD ground state and, within the measurement error, coincides with the corresponding values obtained from LPC spectra. Transitions with the assistance of excited states were not observed, because low intensities of exciting radiation were used in our experiment. In order to observe the transitions with the participation of states with  $n = 2$  and the transitions into the wetting layer, high intensities of excitation ( $> 50$  W/cm<sup>2</sup>) have to be used [7]. However, the interpretation of electron spectra obtained at high intensities within the PL spectroscopy method is not

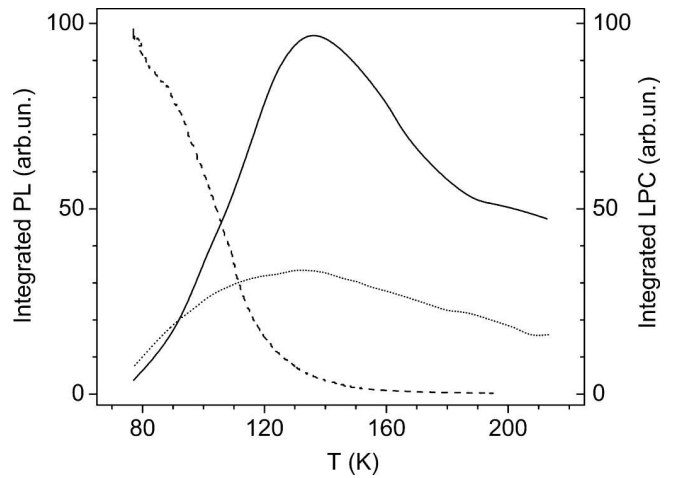


Fig. 6. Temperature dependences of integrated PL (dashed curve) and LPC measured perpendicularly (solid curve) and in parallel (dotted curve) to QD chains for transitions from the QD ground state

correct, because the electron spectra undergo substantial distortions at such deviations from the equilibrium state.

### 3.3. Temperature dependences of photoconductivity and photoluminescence

Electrons and holes generated owing to the interband transitions in QDs are localized at first in the QDs and cannot take participation in charge transfer processes. Those carriers can contribute to the photocurrent, if they are in delocalized states of barrier layers. The carriers can transit there owing to the processes of thermal emission, after having overcome the potential barrier,  $E_a^e$  in height for electrons and  $E_a^{hh}$  for holes (Fig. 5) [10]. In works [22–24], the influence of thermal emission processes on the transverse transport and PL in  $\text{InGaAs}/\text{GaAs}$  heterostructures was studied. It was shown that thermal emission occurs mainly into the WL states, and that interface states and dislocations at interfaces between QDs, the WL, and GaAs are dominating channels of radiationless recombination of electron-hole pairs.

In order to study the thermal emission processes and determine the activation energies  $E_a^e$  and  $E_a^{hh}$ , we measured the temperature dependences of the integrated LPC for specimens with the parallel and perpendicular geometry of contacts and PL (Fig. 6) in the temperature range from 77 to 290 K.

In the temperature measurements, the signal of integrated LPC (Fig. 6) corresponded to transitions with the participation of the QD ground state in the

In<sub>0.4</sub>Ga<sub>0.6</sub>As/GaAs heterostructure. In the temperature range 77–135 K, the exponential growth of the photocurrent corresponding to the basic transition was observed. A further temperature elevation to 240 K was accompanied by a photocurrent reduction. Basing on the relation  $\Delta E_c/\Delta E_v = 0.6$  for the amplitudes of the conduction and valence band mismatches in heterostructures with such a composition [1], the assumption was made that the activation energy for an electron in the heterostructure concerned is lower than that for a hole,  $E_a^e < E_a^{\text{hh}}$ . The shape of the temperature dependence can be explained from the following speculations. If the temperature grows within the interval from 77 to 135 K, it is predominantly electrons that are thermally activated to the WL conduction band (Fig. 5). The increase of the LPC signal at a temperature elevation is explained by the growth of the concentration  $n$  of thermally activated free electrons on the barrier levels, which did not recombine through the radiationless channels into the WL and gave a contribution to the photocurrent. The rate of electron generation for such a process depends on the temperature,

$$\frac{n}{\tau_{\text{esc}}} = A \exp\left(-\frac{E_a^e}{kT}\right). \quad (5)$$

If the temperature continues to increase above 135 K, the process of thermal activation of holes, for which the barrier in the valence band is higher, starts to considerably affect the longitudinal photocurrent signal. The rate  $E_a^{\text{hh}}$  of hole generation to the WL valence band is determined by the relation

$$\frac{p}{\tau_{\text{rec}}} = B \exp\left(-\frac{E_a^{\text{hh}}}{kT}\right). \quad (6)$$

When the holes transit into delocalized states of the WL valence band, they recombine nonradiatively with the participation of interface states or dislocations [24]. If the concentration of thermally activated holes  $p$  increases, the rate of radiationless recombination of electron-hole pairs grows, which results in a photocurrent reduction. In this case, the variation of the electron concentration in the conduction band of barrier layers looks like

$$\frac{dn}{dt} = A \exp\left(-\frac{E_a^e}{kT}\right) - \frac{n}{\tau_{\text{cap}}} - \gamma np, \quad (7)$$

where  $\frac{n}{\tau_{\text{cap}}}$  is the QD electron capture rate, and  $\gamma np$  is the rate of radiationless band-to-band recombination in

the WL. If the stationary process runs at a low temperature, so that the rate of radiationless recombination can be neglected, the expression for the concentration of delocalized (free) electrons looks like

$$\Delta n = A\tau_r \exp\left(-\frac{E_a^e}{kT}\right). \quad (8)$$

Hence, in the temperatures range from 77 to 135 K, when it is predominantly electrons that are thermally activated, the photocurrent density is proportional to the conductivity variation,

$$I_{\text{PC}} \sim \Delta\sigma \sim \mu_e \Delta n = \mu_e A\tau_r \exp\left(-\frac{E_a^e}{kT}\right), \quad (9)$$

where  $e$  and  $\mu_e$  are the charge and the mobility of an electron, respectively.

In the temperature range from 135 to 240 K, the contribution of holes thermally activated from the localized states of the QD valence band becomes appreciable. For this case, the expression for the delocalized (free) hole concentration is

$$\Delta p = B\tau_r \exp\left(-\frac{E_a^{\text{hh}}}{kT}\right). \quad (10)$$

In this range, the expression for the stationary concentration of delocalized electrons can be approximately calculated on the basis of expression (6)

$$I_{\text{PC}} \sim \mu_e n = \frac{\mu_e A \exp(-E_a^e/kT)}{\tau_r^{-1} + \gamma B\tau_r \exp(-E_a^{\text{hh}}/kT)}. \quad (11)$$

Using the obtained expressions (9) and (11) in the corresponding temperature ranges, we approximated the temperature dependence of LPC and obtained the following values of activation energies for thermal emission processes:  $E_a^e = 62 \pm 10$  meV for electrons and  $E_a^{\text{hh}} = 112 \pm 10$  meV for heavy holes.

The described processes of thermal emissions are also responsible for the temperature dependence of the integrated PL (Fig. 6). The PL signal corresponds to radiative recombination transitions with the assistance of the QD ground state of the In<sub>0.4</sub>Ga<sub>0.6</sub>As/GaAs heterostructure. Within the whole temperature interval from 77 to 210 K, the PL quenching with the temperature increase was observed.

The temperature dependence of the integrated PL has a complicated profile, which testifies to the existence of several channels for the thermal emission of nonequilibrium carriers from the QDs. When the heterostructure temperature increases from 77 to 120 K, electrons from

the QD localized states are thermally activated onto delocalized states in the WL or the GaAs barrier. If the temperature grows further, from 120 to 290 K, the thermal activation of holes begins to give an appreciable contribution. An increase in the concentration of thermally activated holes enhances the rate of radiationless recombination between electron-hole pairs, which gives rise, in turn, to a reduction in the number of pairs that can recombine radiatively.

The PL intensity in the case of several channels of PL quenching is described by the following expression [22]:

$$I_{\text{PL}} \sim \frac{I_{\text{max}}}{1 + D \exp(-E_a^e/kT) + F \exp(-E_a^{\text{hh}}/kT)}, \quad (12)$$

where  $D$  and  $F$  are constants. Having approximated experimental data for the integrated PL by dependence (12), we obtained the values for the activation energies of electrons,  $E_a^e = 73 \pm 10$  meV, and heavy holes,  $E_a^{\text{hh}} = 117 \pm 10$  meV. The magnitudes of activation energies derived from the temperature dependences of LPC, PL, and DC coincide with one another to within the calculation error.

The value of activation energy, being summed up with the value for the energy of QD ground state transition (1.235 eV), which was obtained from PL and LPC measurements, gives  $1.43 \pm 0.02$  eV. This energy value is close to the energy of the transition from the heavy hole level in the WL (1.46 eV at 77 K). Hence, it is highly probable that the transport of charge carriers in InGaAs/GaAs structures occurs in the WL plane, where the energy gap width is narrower than that in single-crystalline GaAs, and, respectively, the heights of barriers for electrons and holes are lower. Such a transfer processes can be considerably affected by the processes of radiationless recombination of electron-hole pairs, with the participation of interface and WL dislocation states [25].

#### 4. Conclusions

At low temperatures, the transport of charge carriers in In<sub>0.4</sub>Ga<sub>0.6</sub>As/GaAs heterostructures with QD chains is substantially influenced by the processes of thermal emission and capture of charge carriers, which the InGaAs potential wells are responsible for. In the low-temperature range from 77 to 150 K and when the current in a specimen runs in parallel to QD chains, the mechanism of charge carrier transfer can be described with the help of the Efros–Shklovskii law for the hopping conductivity with a variable hopping distance. The radius of wave function localization  $\xi = 0.5$  nm was calculated. On the other hand, in the case where the current

runs in a specimen normally to QD chains, the temperature dependence of DC can be described in terms of the processes of temperature activation of charge carriers to delocalized states.

Heterostructures In<sub>0.4</sub>Ga<sub>0.6</sub>As/GaAs with QDs revealed the photosensitivity in the intervals of photon energies  $h\nu > 1.22$  eV at 77 K and  $h\nu > 1.17$  eV at 290 K, where single-crystalline GaAs is transparent. It was shown that nonequilibrium charge carriers are generated as a result of interband transitions in the ground state of QD, transitions from  $E_{\text{hh}2}$ -levels into the conduction band continuum, and transitions with the participation of the QD environment. The method of lateral photocurrent spectroscopy was used to determine the energies of those transitions. In PL researches, only the radiative recombination transition with the assistance of QD ground states was observed. The corresponding transition energy coincided with the energy determined from the LPC spectra.

Mathematical equations for the description of the temperature dependence of the photocurrent have been derived. The obtained expressions were used to determine the activation energies  $E_a^e$  and  $E_a^{\text{hh}}$ .

1. D. Bimberg, M. Grudmann, and N.N. Ledentsov, *Quantum Dot Heterostructures* (Wiley, New York, 1999).
2. T. Lundstrom, W. Schoenfeld, H. Lee, and P.M. Petroff, *Science* **286**, 2312 (1999).
3. H. Drexler, D. Leonard, W. Hansen, J.P. Kotthaus, and P.M. Petroff, *Phys. Rev. Lett.* **73**, 2252 (1994).
4. L.I. Glazman and R.C. Ashoori, *Science* **304**, 524 (2004).
5. Q.D. Zhuang, J.M. Li, Y.P. Zeng, L. Pan, Y.H. Chen, M.Y. Kong, and L.Y. Lin, *J. Electron. Mater.* **28**, 503 (1999).
6. M.L. Hussein, W.Q. Ma, and G.J. Salamo, *Mat. Res. Soc. Symp. Proc.* **776**, Q. 11.29.1-11.29.4 (1999).
7. O. Rubel, P. Dawson, S.D. Baranovskii, K. Pierz, P. Thomas, and E.O. Gobel, *Phys. Status Solidi C* **3**, 2397 (2006).
8. Yu.I. Mazur, Zh.M. Wang, H. Kissel, Z.Ya. Zhuchenko, M.P. Lisitsa, G.G. Tarasov, and G.J. Salamo, *Semicond. Sci. Technol.* **22**, 86 (2007).
9. V.V. Strelchuk, Yu.I. Mazur, Zh.M. Wang, M. Schmidbauer, O.F. Kolomys, M.Ya. Valakh, M.O. Manasreh, and G.J. Salamo, *J. Mater. Electr.* **19**, 692 (2008).
10. H.C. Li, J.-Y. Duboz, R. Durek, Z.R. Wasilewski, S. Fafard, and P. Finnie, *Physica E* **17**, 631 (2003).
11. S. Kim, H. Mohseni, M. Erdtmann, E. Michel, C. Jelen, and M. Razeghi, *Appl. Phys. Lett.* **73**, 963 (1998).
12. S.-Y. Lin, Y.-J. Tsai, and S.-C. Lee, *Appl. Phys. Lett.* **78**, 2428 (2001).

13. A. Luque and A. Marti, Prog. Photovolt.: Res. Appl. **9**, 73 (2001).
14. A. Marti, E. Antolin, C.R. Stanley, C.D. Farnen, N. Lopez, P. Diaz, E. Canovas, R.G. Linares, and A. Luque, Phys. Rev. Lett. **97**, 247701 (2006).
15. I. Chu, A. Zrenner, G. Börn, and G. Abstreiter, Appl. Phys. Lett. **76**, 1944 (2000).
16. J.R. Botha and A.W.R. Leitch, Phys. Rev. B **50**, 18147 (1994).
17. A.I. Yakimov, A.V. Dvurechenskii, A.V. Nenashev, and A.I. Nikiforov, Phys. Rev. B **68**, 205310 (2003).
18. A.F.G. Monte, F.V. Sales, and P.C. Morais, J. Phys.: Condens. Matter **21**, 1 (2009).
19. V.A. Romaka, D. Fruchart, L.P. Romaka, A.M. Horyn, O.V. Bovgyra, and R.V. Krayovsky, Ukr. Fiz. Zh. **54**, 1190 (2009).
20. L. Aleiner and B.I. Shkolovskii, Phys. Rev. B **49**, 13721 (1994).
21. N.P. Stepina, E.S. Koptev, A.V. Dvurechenskii, and A.I. Nikiforov, Phys. Rev. B **80**, 125308 (2009).
22. D.P. Popescu, P.G. Eliseev, A. Stintz, and K.J. Malloy, Semicond. Sci. Technol **19**, 33 (2004).
23. W.-H. Chang, T.M. Hsu, C.C. Huang, S.L. Hsu, C.Y. Lai, N.T. Yeh, T.E. Nee, and J.-I. Chyi, Phys. Rev. B **62**, 6959 (2000).
24. J.L. Casas Espinola, M. Dybic, S. Ostapenco, T.V. Torchynska, and G. Polupan, J. Phys.: Conf. Ser. **61**, 180 (2006).
25. S. Sanguinetti, T. Mano, M. Oshima, T. Tateno, M. Wakaki, and N. Koguchi, Appl. Phys. Lett. **81**, 3067 (2002).

Received 01.10.10.

Translated from Ukrainian by O.I. Voitenko

ВПЛИВ ТЕРМІЧНОЇ АКТИВАЦІЇ НОСІЇВ  
 ЗАРЯДУ НА ТЕМПЕРАТУРНІ ЗАЛЕЖНОСТІ  
 ТЕМНОВОГО СТРУМУ, ФОТОПРОВІДНІСТЬ  
 ТА ФОТОЛЮМІНЕСЦЕНЦІЮ ГЕТЕРОСТРУКТУР  
 $\text{In}_{0,4}\text{Ga}_{0,6}\text{As}/\text{GaAs}$  З КВАНТОВИМИ ТОЧКАМИ

*О.В. Вакуленко, С.Л. Головинський, С.В. Кондратенко,  
 І.А. Гринь, В.В. Стрільчук*

## Резюме

У даній роботі досліджено  $\text{In}_{0,4}\text{Ga}_{0,6}\text{As}/\text{GaAs}$  гетероструктуру з ланцюгами квантових точок. Температурними дослідженнями темного струму встановлено існування анізотропії електричних властивостей структури у температурному діапазоні від 77 до 150 К. Обчислено значення величин локалізації хвильової функції та середню довжину стрибка у гетеросистемі. Методом спектроскопії латерального фотоструму та фотолюмінесценції досліджено енергетичну структуру гетеросистеми. Запропоновано теоретичну модель опису температурної залежності латерального фотоструму, в рамках якої з експериментальної залежності отримано значення енергій активації для електронів та важких дірок.